NAVAL
POSTGRADUATE
SCHOOL

MONTEREY, CALIFORNIA

THESIS

SMALL-SCALE AIR-DRIVEN GENERATOR

by

Cory S. McLaughlin

December 2016

Thesis Advisor:	Anthony Gannon
Co-Advisor:	Andrea Holmes

Approved for public release. Distribution is unlimited.

THIS PAGE INTENTIONALLY LEFT BLANK

REPORT DOCUMENTATION PAGE			*Form Approved OMB No. 0704–0188*

1. AGENCY USE ONLY *(Leave blank)*	**2. REPORT DATE** December 2016	**3. REPORT TYPE AND DATES COVERED** Master's thesis	
4. TITLE AND SUBTITLE SMALL-SCALE AIR-DRIVEN GENERATOR		**5. FUNDING NUMBERS**	
6. AUTHOR(S) Cory S. McLaughlin			
7. PERFORMING ORGANIZATION NAME(S) AND ADDRESS(ES) Naval Postgraduate School Monterey, CA 93943-5000		**8. PERFORMING ORGANIZATION REPORT NUMBER**	
9. SPONSORING /MONITORING AGENCY NAME(S) AND ADDRESS(ES) Office of Naval Research, Energy Systems Technology Evaluation Program (ESTEP), under the technical monitoring of Stacey Curtis and Richard Carlin		**10. SPONSORING / MONITORING AGENCY REPORT NUMBER**	
11. SUPPLEMENTARY NOTES The views expressed in this thesis are those of the author and do not reflect the official policy or position of the Department of Defense or the U.S. Government. IRB number ____N/A____.			
12a. DISTRIBUTION / AVAILABILITY STATEMENT Approved for public release. Distribution is unlimited.		**12b. DISTRIBUTION CODE**	

13. ABSTRACT (maximum 200 words)

The purpose of this thesis was to demonstrate the concept of generating electrical energy using only compressed air as a working fluid. Compressed air systems are common on naval installations, posing an enticing opportunity for small-scale electrical generation.

The use of a small turbine, in this case a turbocharger, provided a constant source of shaft power which was used to spin a small permanent magnet motor. With the permanent magnet motor generating alternating current (AC) voltage, a bridge rectifier integrated circuit (IC) was used to rectify the voltage to direct current (DC). The electricity generated was then stored in a 16-volt supercapacitor.

While testing the system, it was discovered that more shaft power could be produced if atmospheric air was entrained into the turbine housing inlet. The effect was similar to an ejector, which is commonly used on aircraft engines to increase thrust.

This research demonstrated the feasibility of combining commercially available components to harness compressed air in order to generate electricity on a small scale. This system could be utilized to offset power spikes associated with heavy equipment startup, or as an always-on emergency backup system for critical components.

14. SUBJECT TERMS compressed air, energy storage, turbocharger, permanent magnet motor, small scale, electrical generation, supercapacitor			**15. NUMBER OF PAGES** 63
			16. PRICE CODE
17. SECURITY CLASSIFICATION OF REPORT Unclassified	**18. SECURITY CLASSIFICATION OF THIS PAGE** Unclassified	**19. SECURITY CLASSIFICATION OF ABSTRACT** Unclassified	**20. LIMITATION OF ABSTRACT** UU

THIS PAGE INTENTIONALLY LEFT BLANK

SMALL-SCALE AIR-DRIVEN GENERATOR

Cory S. McLaughlin
Lieutenant, United States Navy
B.S., United States Naval Academy, 2010

Submitted in partial fulfillment of the
requirements for the degree of

MASTER OF SCIENCE IN MECHANICAL ENGINEERING

from the

**NAVAL POSTGRADUATE SCHOOL
December 2016**

Approved by: Anthony Gannon
                    Thesis Advisor

                    Andrea Holmes
                    Co-Advisor

                    Garth Hobson
                    Chair, Department of Mechanical and Aerospace
                    Engineering

THIS PAGE INTENTIONALLY LEFT BLANK

ABSTRACT

The purpose of this thesis was to demonstrate the concept of generating electrical energy using only compressed air as a working fluid. Compressed air systems are common on naval installations, posing an enticing opportunity for small-scale electrical generation.

The use of a small turbine, in this case a turbocharger, provided a constant source of shaft power which was used to spin a small permanent magnet motor. With the permanent magnet motor generating alternating current (AC) voltage, a bridge rectifier integrated circuit (IC) was used to rectify the voltage to direct current (DC). The electricity generated was then stored in a 16-volt supercapacitor.

While testing the system, it was discovered that more shaft power could be produced if atmospheric air was entrained into the turbine housing inlet. The effect was similar to an ejector, which is commonly used on aircraft engines to increase thrust.

This research demonstrated the feasibility of combining commercially available components to harness compressed air in order to generate electricity on a small scale. This system could be utilized to offset power spikes associated with heavy equipment startup, or as an always-on emergency backup system for critical components.

THIS PAGE INTENTIONALLY LEFT BLANK

TABLE OF CONTENTS

LIST OF FIGURES

LIST OF ACRONYMS AND ABBREVIATIONS

AC	alternating current
ATM	atmospheres
CAES	compressed air energy storage
DC	direct current
ESOI	energy stored on invested
IC	integrated circuit
RC	radio controlled
RPM	revolutions per minute
UPS	uninterruptible power supply

THIS PAGE INTENTIONALLY LEFT BLANK

ACKNOWLEDGMENTS

I'd like to thank both of my advisors for their time and guidance through this project. I'd also like to thank my wife and son for their patience while I was working late and on weekends.

THIS PAGE INTENTIONALLY LEFT BLANK

I.   INTRODUCTION

The purpose of this thesis is to demonstrate the concept of producing electrical power on a small scale using only compressed air as a working fluid. A brief background is discussed regarding the motivation for this research, as well as the current state of the art in generating power from stored compressed air.

A.   WHAT IS CAES AND WHY USE IT?

Compressed air energy storage, or CAES, is the concept of using renewable energy sources to power air compressors in order to store large amounts of compressed air for future use in either industrial applications or power generation [1]. There are many potential uses of CAES for the Navy, particularly ashore. The Secretary of the Navy has promulgated five goals with respect to energy, the second of which is to "increase alternative energy ashore" [2]. This goal is intended to be met by the year 2020, with the primary sources as solar and wind [2]. With the upswing of renewable energy sources throughout the Navy's shore installations, energy storage will become a key factor. Diversifying energy storage options will allow for reduced costs, both capital and operational, which directly contributes to achieving the Secretary of the Navy's energy goals. CAES in particular can have a very deep depth-of-discharge over many discharge cycles, which when paired with the relatively low energy cost to install a CAES system can result in a very high ratio of energy stored over the lifetime to the energy required to install [3]. Barnhart and Benson refer to this ratio as the energy stored on invested, or ESOI [3]. Additionally, task-tailored energy storage using a multi-physics approach should produce a more comprehensive and effective energy storage system [4].

B.   WHY SMALL-SCALE POWER GENERATION?

If compressed air stored at normal industrial pressures of about 10 ATM can be converted from compressed air energy to electrical energy, it can serve as a source of electrical power. The utility of a CAES system could increase. It

could be used to charge a battery or supercapacitor bank used in microgrid systems. The additional electrical power produced could be enough to offset the power required to start up heavy machinery, or power an Uninterruptible Power Supply (UPS) system, or simply provide short-term emergency power. Small-scale compressed air systems are common in Navy shore facilities, particularly in industrial or maintenance facilities for use with pneumatic tools. The common occurrence of these systems in naval facilities provides ample opportunity for them to be used as an energy storage media. Additionally, a diversified and distributed power generation portfolio should help improve energy security by reducing the dependence on any one mode of generation.

C.   CURRENT STATE OF THE ART

CAES is currently only used in large, utility-scale applications [5]. These systems closely resemble normal utility scale power plants in that they still utilize a Brayton cycle to produce the power [5,6]. The difference between the two is that CAES uses renewable energy sources to pump air into large caverns where is it stored for later use. In order to recover the energy stored in the compressed air, heat must be added. This usually involves a combustion process. When the utility power grid experiences spikes in demand, the utility can then release some of the stored compressed air into the Brayton cycle to give it a quick boost in power output [6]. The limiting factor for applications of this scale is geography. Utility providers wishing to utilize CAES depend on having the right geographical features in their service area, whether it is a salt dome or a large underground cavern that can be sealed [5]. These geographical limitations preclude the use of CAES in any application for the Navy.

D.   ENABLING TECHNOLOGIES FOR SMALL-SCALE CAES

Although the use of a traditional CAES system is not practical for the Navy, there are a few key enabling technologies which may allow for future widespread small-scale applications. Some of the primary enabling technologies, which are discussed in further detail later in this thesis, include automobile

turbochargers and small permanent magnet motors commonly used in remote controlled devices. The pairing of these two technologies is currently being utilized in the formula one racing community [7] to charge batteries or supercapacitors used to provide both boost to the compressor end of the turbocharger at low revolutions per minute (RPM) as well as to power electric motors which move the car at low speeds. Essentially the formula one community pairs turbochargers and electric motors to make their cars hybrid [7].

E.   PROPOSED DESIGN CONCEPT

Figure 1 depicts a simple schematic for the overall system proposed in this thesis. Each of the individual components seen in the figure, with the exception of the compressed air, are discussed further in Chapter III. This proposed design shows how it may be possible to generate and store electrical energy using previously stored compressed air by employing the key enabling technologies discussed earlier.
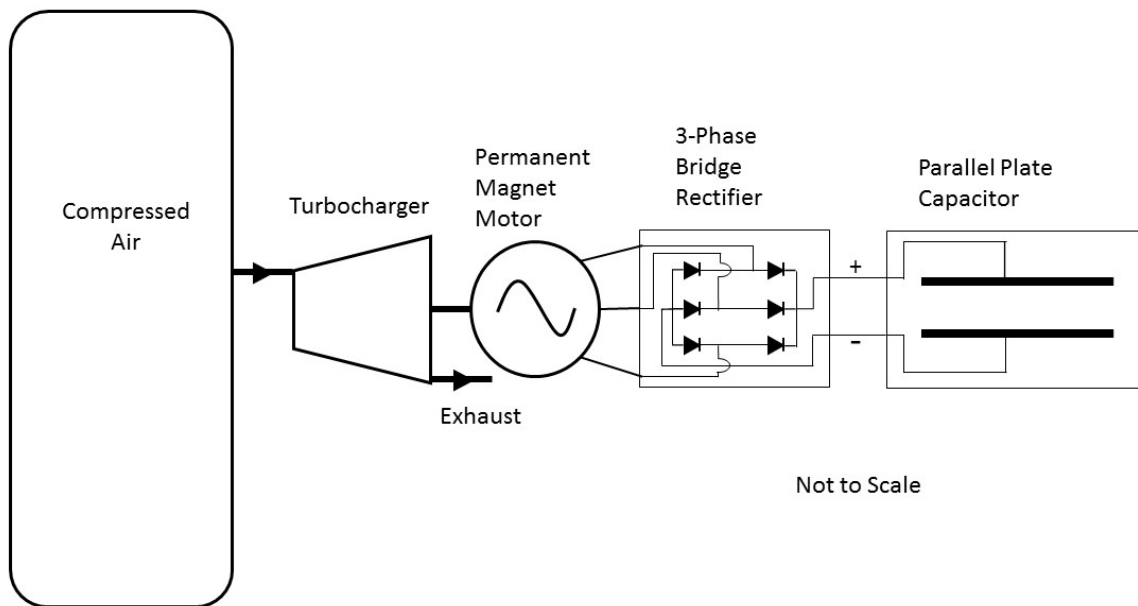
Figure 1. Proposed Design Concept

THIS PAGE INTENTIONALLY LEFT BLANK

II. THEORY

Just as there are a few key enabling technologies that allow this system to work, there are a few key theoretical concepts behind the enabling technologies. These concepts are compressible flow, turbine theory, ejector theory, and permanent magnet motors and generators. This chapter briefly discusses these concepts.

A. COMPRESSIBLE FLOW

The concept of compressible flow is important to this project because of the nature of the working fluid, compressed air. Compressible flow problems typically deal with high velocities, which for air and other gasses can be generated with relatively low pressure ratios [8]. One of the main effects of compressible flow which is a key concern for this project is the phenomenon of choking. Choking occurs when an internal flow reaches the speed of sound, or the sonic condition. Choked conditions represent the maximum mass flow rate for any given stagnation temperature and pressure, and throat area. Since the system would be utilizing pipes of relatively small diameter, 19 mm (3/4 inch) and smaller which is typical of a shop compressed air systems, and the flow would be an internal flow bound for a turbine, care had to be taken to maximize the mass flow rate of compressed air into the turbine inlet. To calculate the maximum mass flow rate of air through any one of the components equation one was used from [8],

$$\dot{m}_{max} = \frac{0.6847 P_0 A^*}{\sqrt{R T_0}},$$ (1)

where P_0 and T_0 are the stagnation pressure and temperature, R is the gas constant for air, and A^* is the cross sectional area of the component. Since the stagnation pressure and temperature through any given component cannot be changed during a discharge without an external source of energy, the cross

sectional area became the critical variable, particularly when sizing the compressed air fittings.

B.   TURBINE THEORY

Turbines are rotating machinery designed to extract energy from a working fluid [8] by lowering the enthalpy. There are two main categories of turbine, reaction and impulse. The flows across these turbines can be in either the radial or axial directions, or a mix of the two. For this project, a radial inflow reaction turbine was used.

C.   EJECTOR THEORY

Ejectors are non-moving pieces of machinery commonly used in the aerospace industry to increase thrust out of gas turbine engines. Typical ejectors mix two fluid streams through the viscous interaction at the boundary of the primary stream and the secondary stream [9]. One of these streams is usually a high velocity high temperature primary stream out of the core of the gas turbine engine. The secondary stream can either be the bypass flow from the bypass duct in the engine, or atmospheric air. The mixing of the two streams results in an increased mass flow rate, which directly affects the thrust produced by the engine. Ejector theory is relevant to this project due to the nature of the working fluid. The circumstances surrounding the discovery of the relevance are discussed in Chapter III. For this project, ejector theory produced a twofold effect by both increasing the mass flow rate over the turbine and increasing the enthalpy of the working fluid entering the turbine. The adiabatic expansion of the compressed air into the turbine inlet produces a very cold jet of air with low enthalpy. When the cold jet mixes with the warm atmospheric air, the enthalpy upstream of the turbine is higher, which allows the turbine to be more effective. The combined effect was a noticeable increase in shaft power produced by the turbine.

D.   PERMANENT MAGNET MOTORS AND GENERATORS

The governing principle behind electric motors and generators is Faraday's Law of Electromagnetic Induction. This law states that a voltage will be induced in stationary wire coils proportional to the rate of change in magnetic flux perpendicular to the coils [10]. Permanent magnet motors are a good example of the application of Faraday's law, as the array of magnets are rotated around the wire coils the magnetic flux constantly changes, producing a sinusoidal voltage waveform. The wire coils are wound around a fixed support called a stator, which can either be an iron core or another permanent magnet, and the number of individual wire loops wound around the stator arms dictates how many phases the machine will have. Faraday's law also states that the voltage induced by the changing magnetic flux depends upon how many times the wire is wound around the stator, the more windings the higher the voltage as seen in equation two from [10],

$$e = N\frac{d\Phi}{dt},$$
(2)

where N is the number of windings around the stator. Equation two shows that the voltage generated is a function of the changing magnetic flux, ϕ, which is directly related to the motion of the magnets. So the faster the magnets rotate, the more voltage is generated. Whether the machine is a motor or a generator will depend on what form of energy is supplied to it. If mechanical energy is supplied in the form of shaft power to rotate the magnetic field, it is a generator. Conversely, if electrical energy is supplied to the wire coils an electromagnetic force will be induced and the machine will act as a motor. This is a unique advantage for permanent magnet motors as no external source of energy is needed to induce the magnetic field.

THIS PAGE INTENTIONALLY LEFT BLANK

III.   DESIGN ELEMENTS

As mentioned earlier, there are some key enabling technologies which allow for small-scale power generation using only compressed air. These technologies—and the reasons they were included in the design—are discussed in further detail in this chapter. The discussion proceeds piece by piece through the schematic shown previously in Figure 1 from Chapter I.

A.   SMALL-SCALE TURBINE

The decision to use a small-scale turbine was made on the basis of simplicity. In order to extract work from the compressed air, either a piston or turbine was needed to produce shaft power. If a piston were to be used, the flow of the compressed air would have to become cyclical instead of constant, as the piston would have to cycle back to its original position and a timed valve system would also need to be incorporated. A turbine provided a much simpler, constant source of shaft power to the permanent magnet motor. Another reason a small turbine was chosen over a piston system was the issue of lubrication. A piston driven system would have many moving parts, which would need a constant source of lubrication, whereas a small turbine wheel on a shaft only has one moving part, the shaft. The rotating turbine shaft necessitates the use of bearings, either journal or ball, to keep the shaft balanced as well as free to rotate. Journal bearings would still require some source of lubrication to function properly, but ball bearings would only require an initial application of lubrication with the occasional reapplication.

The decision to use an automobile turbocharger as the small-scale turbine was also made on the basis of simplicity, as well as cost. Turbochargers are a very well established and widely used technology, which made the purchasing process very easy in this case. Commercially available turbochargers also come preassembled with the bearings, turbine, shaft, and turbine housing. With everything on the turbocharger already assembled, removing the compressor

housing to expose the end of the shaft so that it could be connected to the shaft of the permanent magnet motor and attaching the compressed air line to the turbine housing inlet were the only modifications required.

Garrett, owned by Honeywell, produces a wide range of turbochargers designed for both gasoline engines as well as diesel engines [11]. Two turbochargers were tested, specifically the GT0632SZ and the GT2554R. The GT0632SZ was originally chosen, as it is the smallest turbocharger produced by Garrett. At first it seemed to be the best choice as it had a small wheel diameter of 30mm and would produce very high RPM. Although the turbine was capable of producing very high RPM with no load on the shaft, the GT0632SZ was limited to a mass flow rate of only 0.023 kg/s (3 lbm/min) which when combined with the small wheel diameter, wasn't capable of producing enough torque or shaft power to spin any of the motors selected for testing. Even though the oil inlet and outlet were sealed with oil inside to constantly lubricate the journal bearing, the high contact area associated with a journal bearing produced too much resistance which further reduced the shaft power available to spin the motor. The GT2554R however, is the smallest ball bearing turbocharger produced by Garrett [11]. With a wheel diameter of 53mm and a maximum mass flow rate at just below 0.113 kg/s (15 lbm/min), this turbocharger was capable of producing much more torque and shaft power, and did not require a constant source of lubrication. Thus, because of the increased torque and the ball bearings, the GT2554R was used in the final design.

It was discovered during testing of the GT2554R that more shaft power would be produced if the wastegate was opened and the inlet plate with the compressed air fitting attached was offset from the turbine housing inlet, as seen in Figures 2 and 3. This seemed at first to be counter-intuitive, but upon further consideration it became clear that atmospheric air was being entrained into the turbine housing through the gaps between the inlet plate and the turbine housing inlet. The reason for this was because the static pressure inside the turbine housing was less than atmospheric pressure, thus creating a pressure gradient.

10

With no physical boundary in this pressure gradient, the atmospheric air was free to flow into the turbine housing with the air jet exiting the compressed air fitting. This phenomenon is known as entrainment and is sometimes used in industrial devices called ejectors, which increase the mass flow rate. Modeling of this was done using ANSYS CFX which can be seen in Appendix A. ANSYS CFX calculated the mass flows from the compressed air fitting and outlet as 0.133 kg/s and 0.1697 kg/s respectively, indicating an increase of 28%.
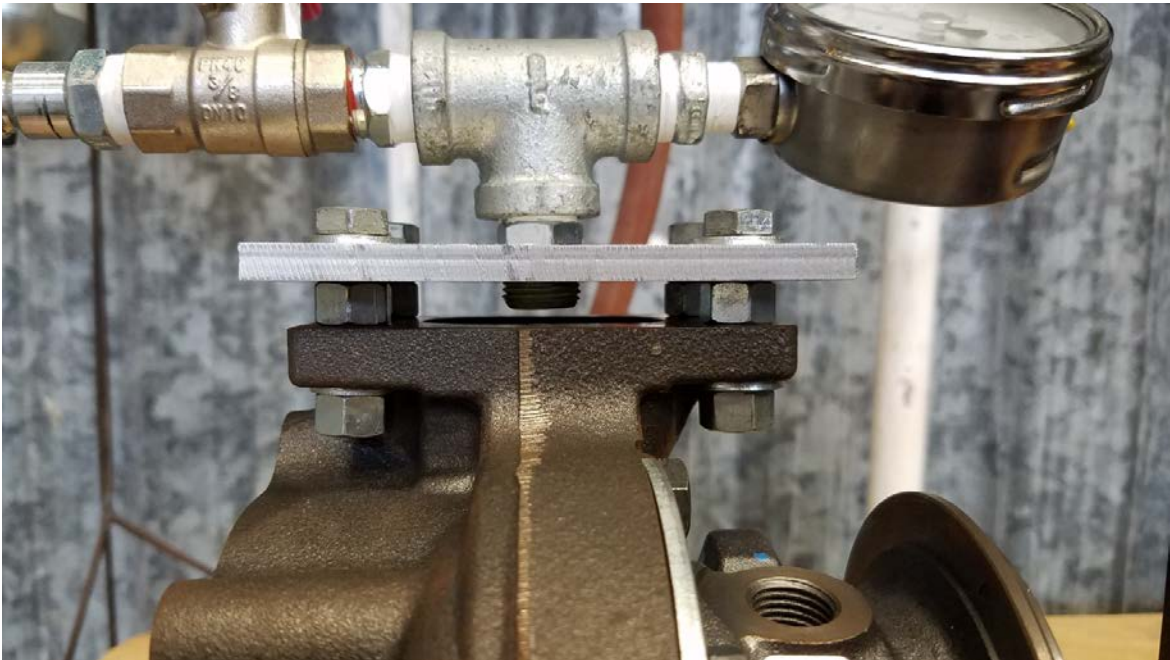
Figure 2. Turbine Housing Inlet
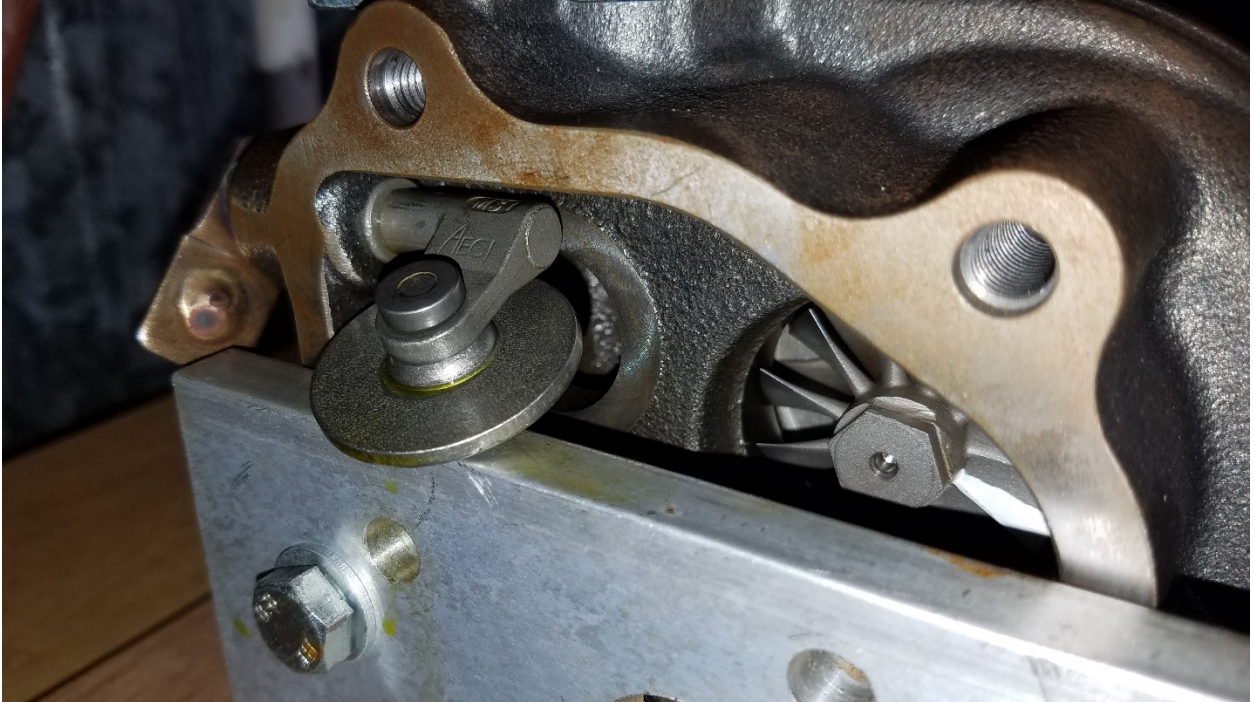
Figure 3. Turbine Exit with open Wastegate

B.   PERMANENT MAGNET MOTORS

There are many different types of permanent magnet motors commercially available today. The decision to use a permanent magnet motor was also based on simplicity. Permanent magnet motors do not require an excitation voltage to induce the magnetic field, the magnetic field is always present. As the magnetic field is always present, no external source of electricity was needed, nor would any electrical energy needed to be taken from the generation to maintain the magnetic field, all of the electricity generated could be used to charge the capacitor. Permanent magnet motors can be used in many different applications, but the small scale of this project guided the search to motors used in radio controlled devices. Several different types of motors were considered for this project, primarily boat and helicopter motors. These types of motors are primarily used by hobbyists, but the RC industry has driven the demand for more advanced small permanent magnet motors, which also made these motors an ideal choice for this research.

The specific models looked at were the P1515-B22 and P1527-B15 by Poseidon, and the HKIII-4035-560 by Scorpion. Boat motors seemed to be the best option at first, as they were capable of handling very high speeds at around 50,000 RPM which is similar to the typical operational RPM of turbochargers. This turned out to be the wrong approach, as the turbocharger selected would never be capable of spinning this type of motor that fast. The reason for this is once an electrical load was placed on the motor the induced torque was too high for the turbine to overcome, and the turbine would stop spinning. Helicopter motors turned out to be a good fit for this application. One of the main reasons a helicopter motor was used instead of a boat motor was the difference in the KV values. The KV rating of an RC motor is defined as the number of RPM the motor will produce per volt supplied. The assumption that the inverse of the KV value would be the voltage generated by the RPM supplied to motor was made, which will be discussed in the next chapter. The boat motors tested for this project had KV ratings of 1500 and 2550, whereas the helicopter motor used in the final design had a KV value of 560, which meant more open circuit voltage could be generated. When it was realized that the maximum RPM of the motor was no longer a limiting factor, the focus shifted to producing the most AC voltage out, which the helicopter motor did. The model used in the final design was the Scorpion HKIII-4035-560KV, shown in Figure 4.

Figure 4. Scorpion HKIII-4035-560KV. Source: [12].

C.   BRIDGE RECTIFIER

A bridge rectifier is an integrated circuit that rectifies incoming AC voltage into DC voltage. This is done by using two diodes in series per phase as seen in Figure 5.
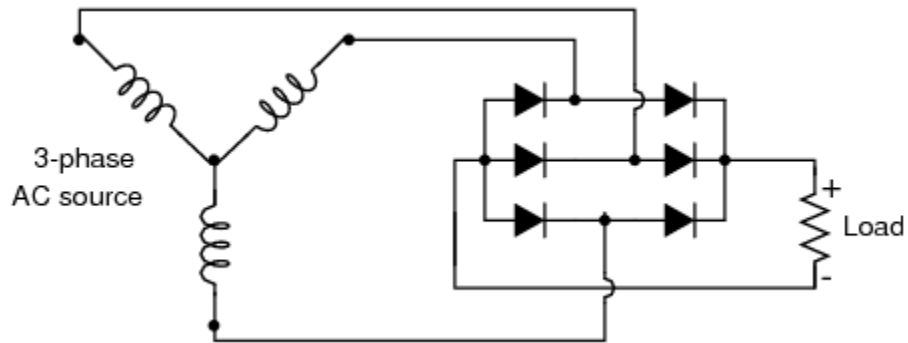
Figure 5. Three Phase Full Wave Bridge Rectifier Circuit. Source: [13].

The need for a rectifier was based on the needed voltage to charge the capacitor, which was DC. With the motor supplying AC voltage, something was needed to convert it to DC, which a bridge rectifier is designed to do very simply. The specific bridge rectifier used for this project was the IXYS VUO86-16NO7-481366 three phase bridge rectifier shown in Figures 6 and 7 showing which leads are the positive and negative terminals and the other three corresponding to each of the three phases.

Figure 6. IXYS Three Phase Bridge Rectifier. Source [14].
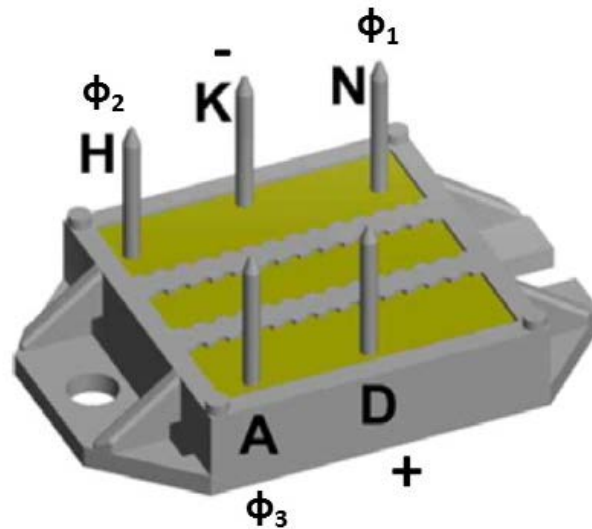
Figure 7. Rectifier Chip with Labeled Leads. Adapted from [15].

D. SUPERCAPACITOR

It was decided to use capacitors for this research project because of their ability to charge faster than batteries. Unlike batteries, capacitors are not limited by the speed of any chemical reaction. This allows the energy generated by the motor to be more efficiently stored. More importantly, it means the motor would need to be running for less time, which means the compressed air would need to

be flowing over the turbine for less time, which means greater overall system efficiency.

The supercapacitor chosen for this research was a Maxwell BMOD0500 P016 B02 16 volt 500 farad capacitor shown in Figure 8. Typical uses for this particular model are in wind turbines, transportation, heavy industrial equipment, and UPS systems [16], all of which made it an ideal choice for this project in addition to its being rated for up to one million duty cycles. Another reason it was chosen was that it was already available on hand.

Figure 8. Maxwell 16V Capacitor. Source: [16].

E.   FINAL DESIGN

With all of the individual components selected, the next challenge was to assemble to whole system. The challenge here was connecting the turbine shaft to the motor shaft. A means of mechanically attaching the two shafts was needed that would be both forgiving and strong enough to withstand the high RPMs and the opposing torques supplied by the turbine and motor. This coupling also needed to be able to be used with different shaft diameters, as different motors were going to be tested as well as different turbochargers. In the end, a simple

high speed flexible coupling seen in Figure 9, consisting of 5 mm (3/16 inch) diameter clear vinyl hose and two hose clamps provided a solution that was capable of withstanding the operating rigors of the system as well as allowing for slight misalignment between the two shafts. The motor was mounted to a flat piece of carbon fiber seen in Figure 9 which had holes drilled through it for the mounting screws and motor shaft, as well as additional holes to mount it to something else. This ended up working very well, as the geometry for mounting holes on most RC motors is standardized, so the piece of carbon fiber was able to be used for all of the motors tested. For the electrical components, ten gauge wire was used to connect both the motor to the bridge rectifier, and the bridge rectifier to the capacitor. The wires were soldered to the appropriate leads on the rectifier chip, which was mounted on a solderless breadboard. The turbocharger, motor, and breadboard were all mounted to a common piece of wood, which provided a flat sturdy surface to hold everything in place during operation. The final assembly of the system can be seen in Figure 10.
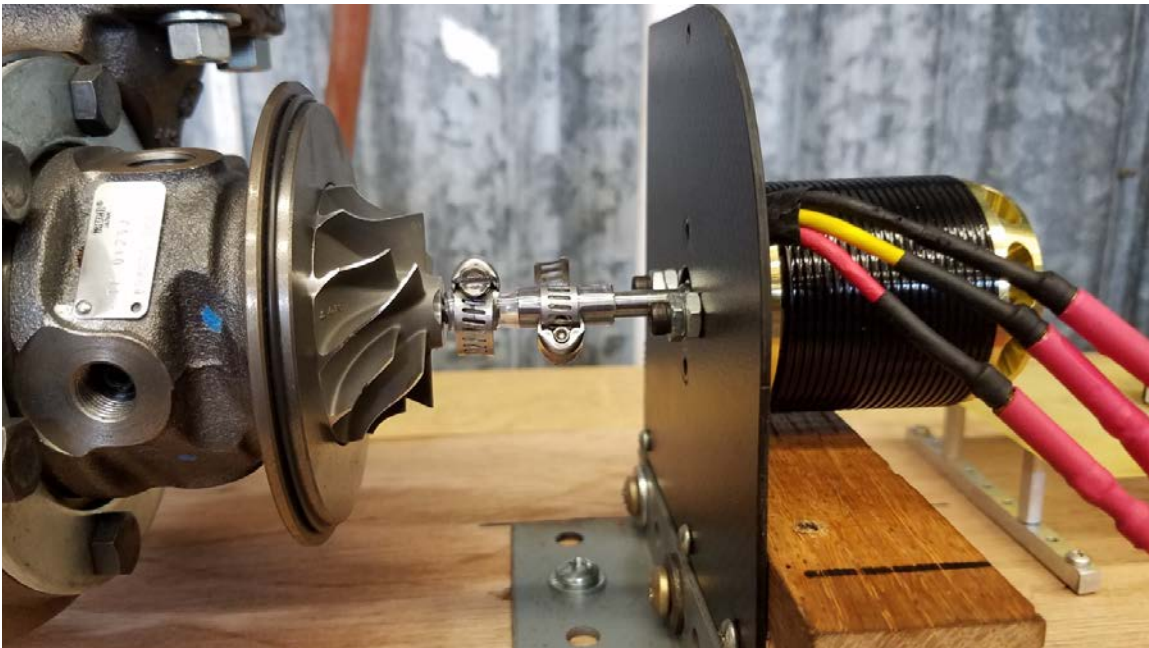
Figure 9. High Speed Flexible Coupling
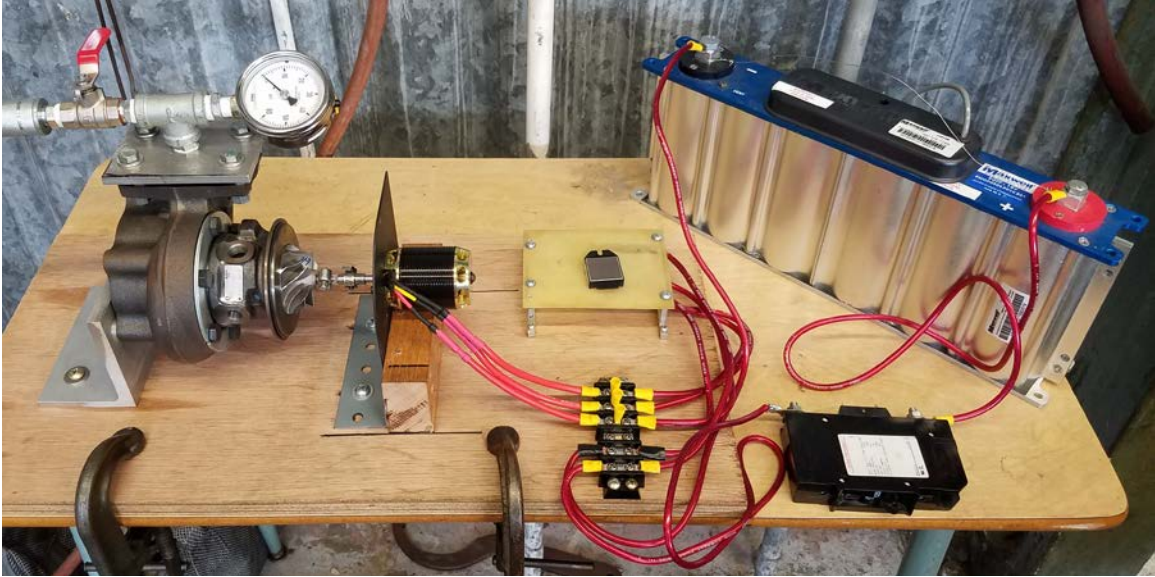
Figure 10.   Final Test Set-up

IV. TEST RESULTS

Initial tests were conducted in order to first confirm that using a permanent magnet motor would in fact produce AC voltage. This was done by connecting a mechanical router to the motor which was also connected to an oscilloscope to read the AC waveform. The resulting waveform can be seen in Figure 11.

Figure 11.   AC Waveforms from Poseidon RC Boat Motor

With the confirmation that a permanent magnet motor could be used as a generator, the focus was shifted to spinning the motor using the turbocharger. Only the Scorpion helicopter motor was tested with the turbocharger, because it had a lower KV value so it required fewer RPMs to produce similar voltages, and it also required less torque to begin spinning. Several tests were conducted to determine just how much open circuit voltage the motor could produce, and how many RPM would be produced by the turbocharger subjected to a load. As

mentioned in Chapter III, it was discovered that a significant increase in shaft power could be achieved by entraining air into the turbine inlet. The open circuit voltage measured on the oscilloscope was increased from approximately six volts to about 10 volts for the Scorpion motor.

With what seemed to be a maximum open circuit voltage and RPM produced by the system, testing was then shifted to actually charging the supercapacitor. A high current breaker switch was installed to be able to electrically isolate the capacitor once it was charged by physically breaking the circuit. Three charging cycles were conducted. For two of the charging cycles the DC voltage across the capacitor was recorded at regular time intervals as well as the frequency from the oscilloscope so that RPM could be calculated for every DC data point using equation three from [10]

$$S = \frac{120f}{n}, \tag{3}$$

where S is RPM, f is the frequency recorded from the oscilloscope, and n is the number of magnetic poles in the motor, which for the motor used is 10. The tabulated data for both charging cycles can found in Appendices B and C, the charging curves built from this data are shown in Figures 12 and 13.
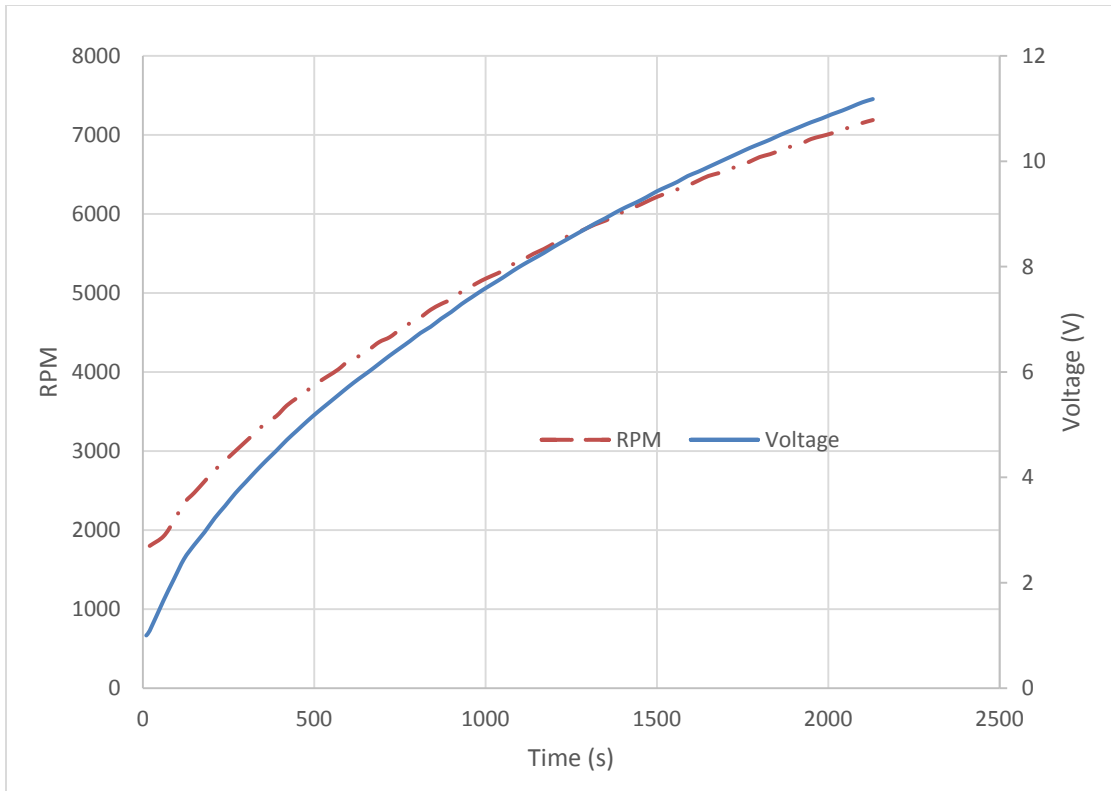
Figure 12.   Curves for the First Charging Cycle
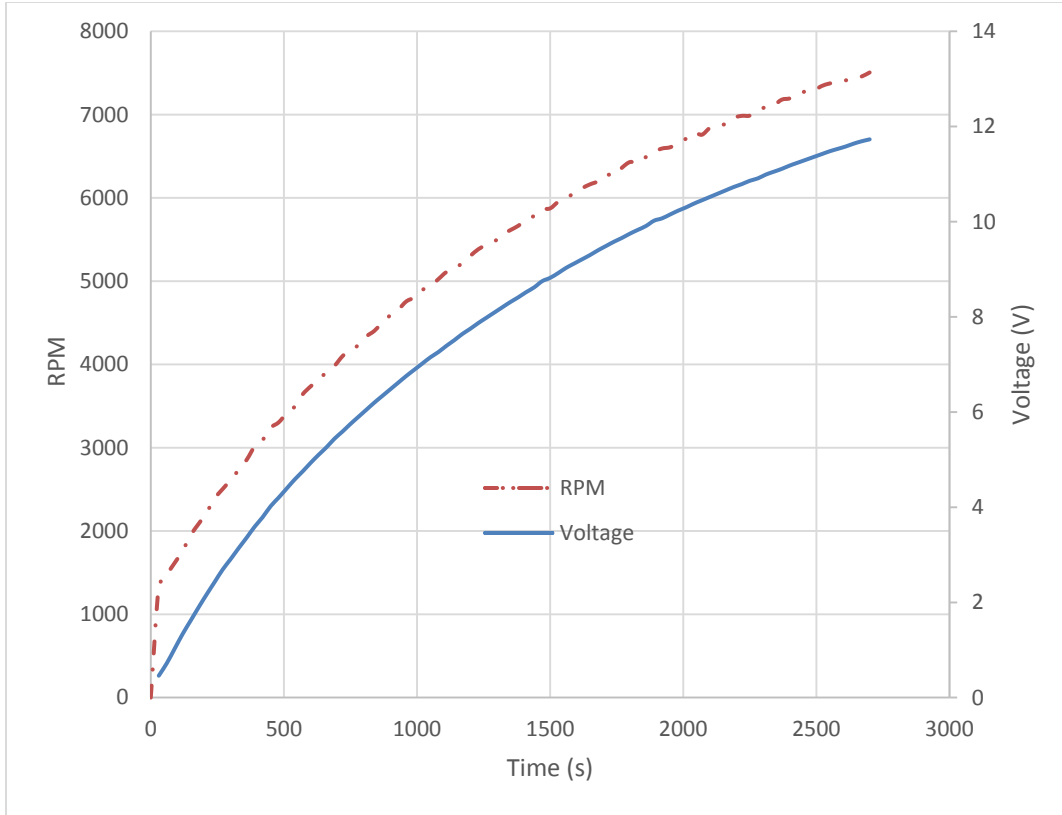
Figure 13.   Curves for the Second Charging Cycle

These two charging curves are typical for capacitors, as the time rate of change of the voltage on the capacitor decreases as more charge is placed on the capacitor. For both charging cycles, the motor reached a final RPM of just over 7000 which is well below the motors rating of about 20,000 RPM.

With the voltage and time measured to charge the capacitor, the current and energy stored could then be calculated using Equation four from [17]

$$I(t) = C\frac{dV}{dt},$$ (4)

for the current where C is the capacitance of the capacitor, and Equation five from [18]

$$W = \frac{1}{2}CV^2$$ (5)

22

for the energy stored. These values were then plotted against time and can be seen in Figures 14 and 15 for the first charging cycle, and Figures 16 and 17 for the second charging cycle.
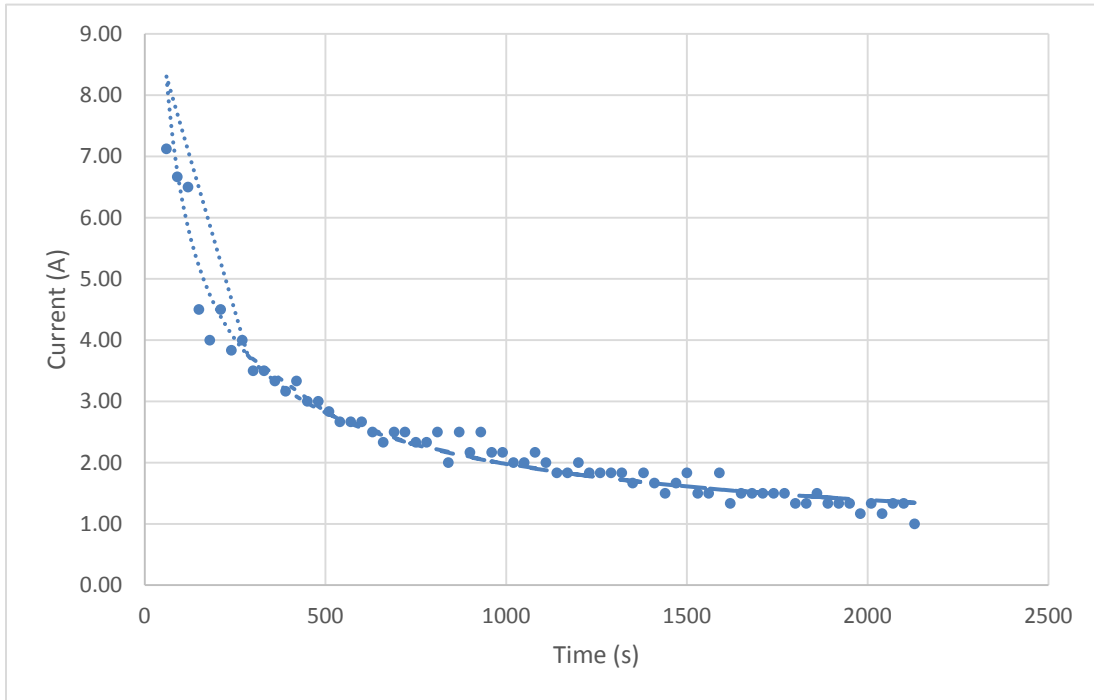
Figure 14.   Current vs. Time for the First Charging Cycle
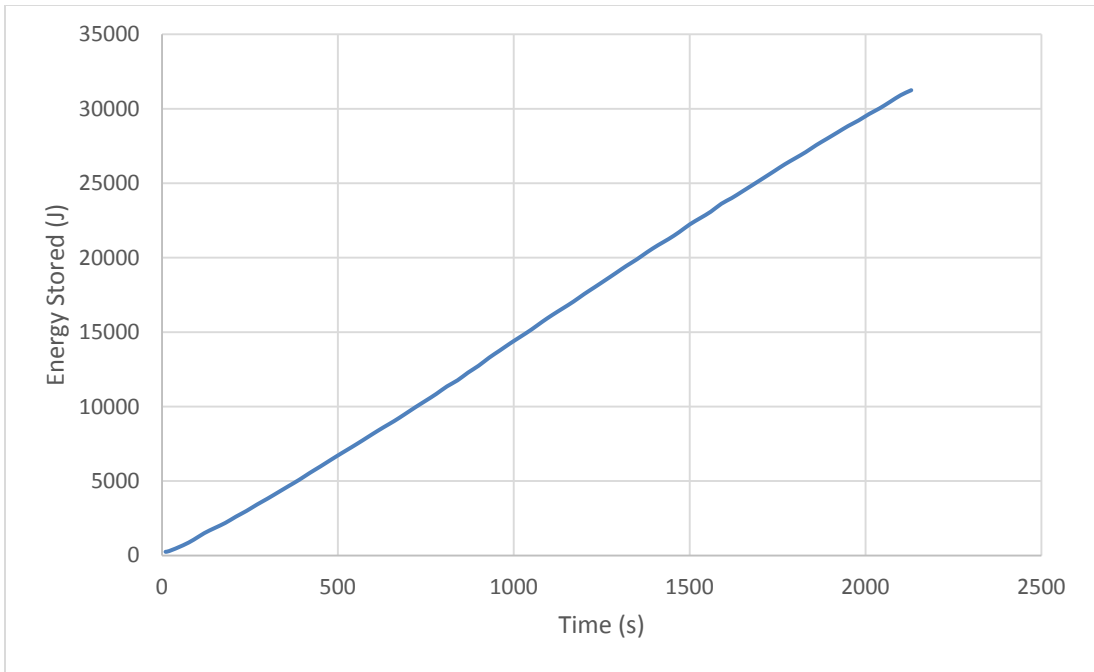
Figure 15.   Energy Stored vs. Time for the First Charging Cycle
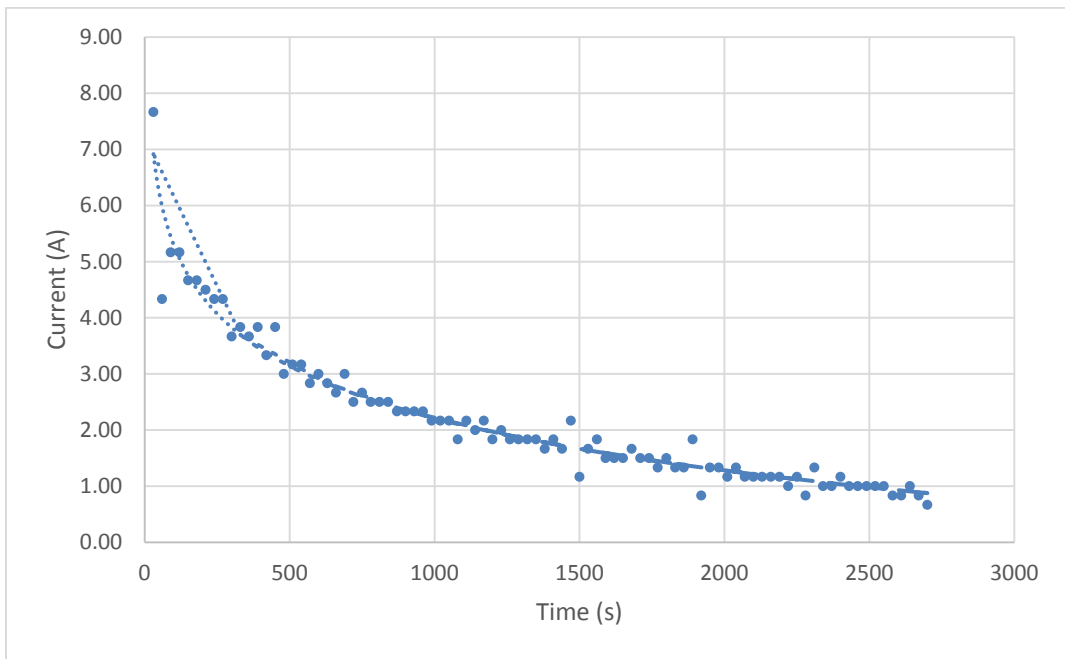
Figure 16.   Current vs. Time for the Second Charging Cycle
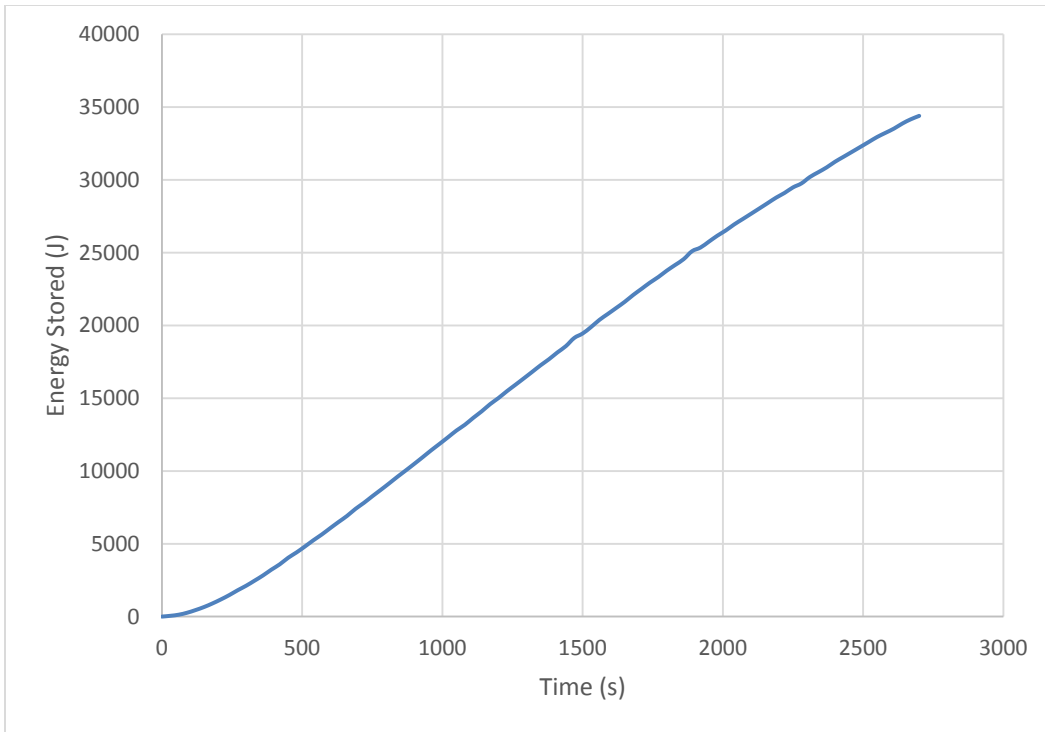
Figure 17.   Energy Stored vs. Time for the Second Charging Cycle

These curves are also typical of charging a capacitor, as the current is directly proportional to the time rate of change of voltage on the capacitor. Both charging cycles produced over 30 kJ of energy stored on the capacitor, which in electrical form can be used in many different ways.

The third charging cycle was more of an endurance test for the system to see how high the capacitor could be charged using this configuration. The results can be seen in Figures 18 and 19, which show a final DC voltage across the capacitor at 15 volts, and a final frequency of 775 Hz or about 9300 RPM which is well below the recommended speed for the motor.
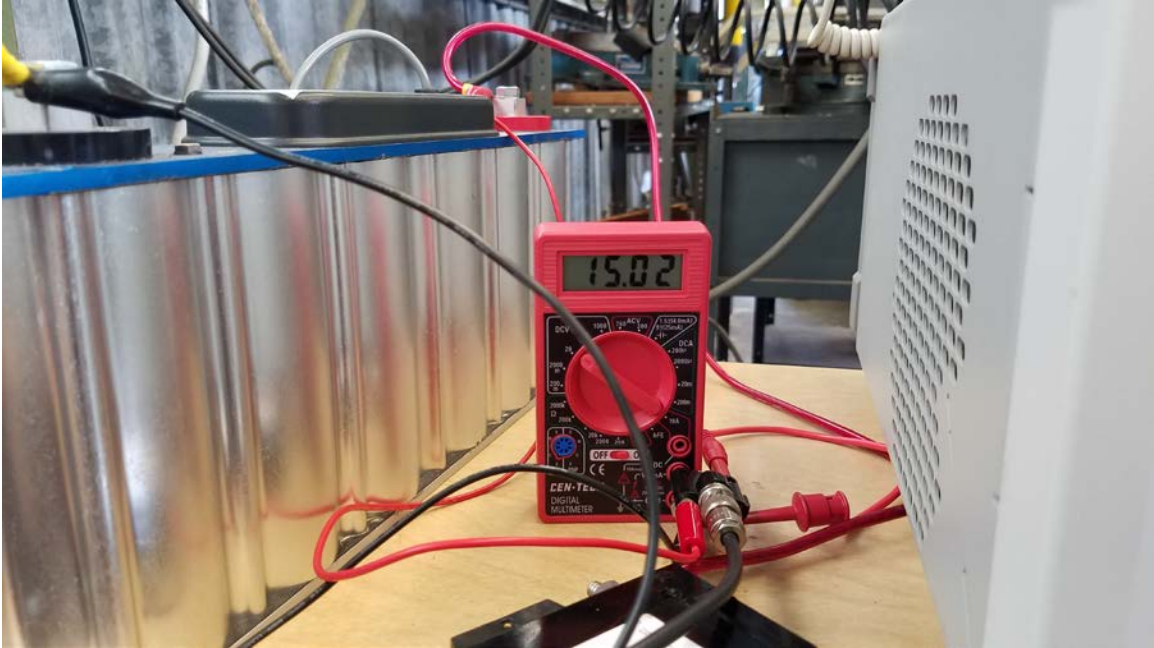
Figure 18.   Final DC Voltage across the Capacitor
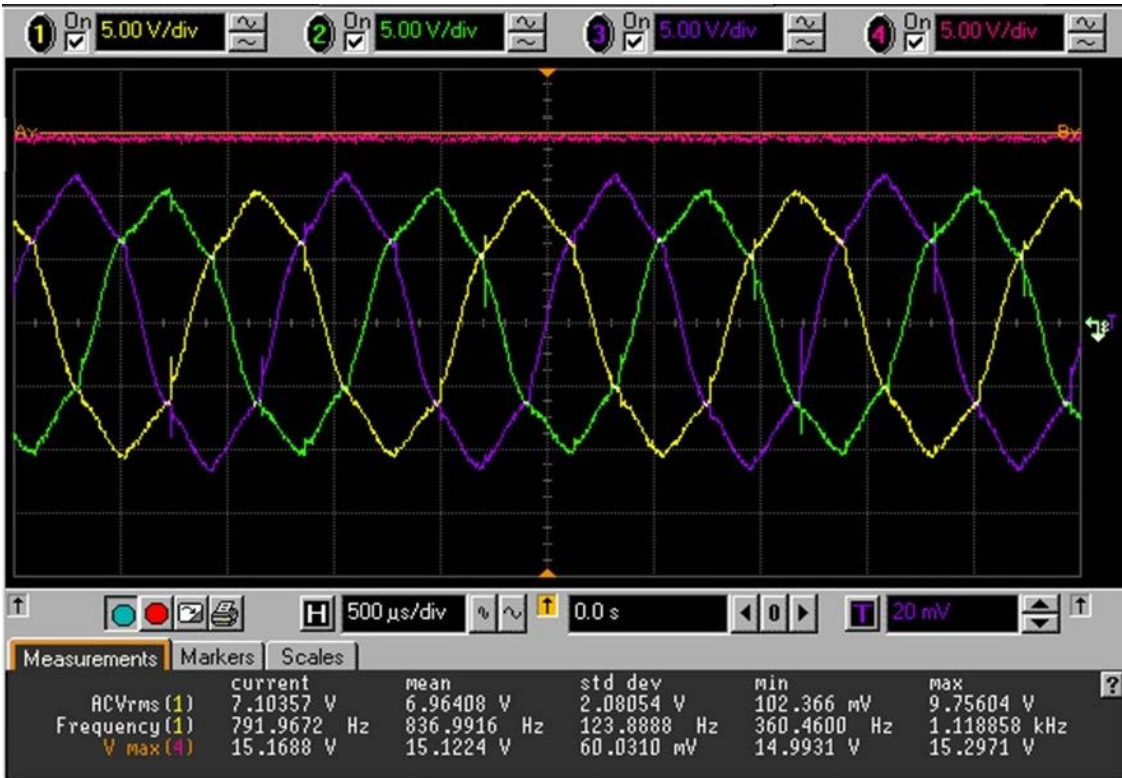
Figure 19.   Final DC Voltage Reading on the Oscilloscope

In Chapter III, the assumption regarding the motors KV value was discussed. To test this assumption, the calculated RPM was then divided by the KV value of the motor which was 560, and the result was plotted on the same graph as the recorded DC voltages on the capacitor. As seen in Figures 20 and 21, the assumption turned out to be reasonable, as the difference between the assumed source voltage on the motor and the DC voltage across the capacitor was essentially constant. The roughly 1.6 volt difference is accounted for by the 0.8 volt drop across each of the diodes per phase in the rectifier chip [15].
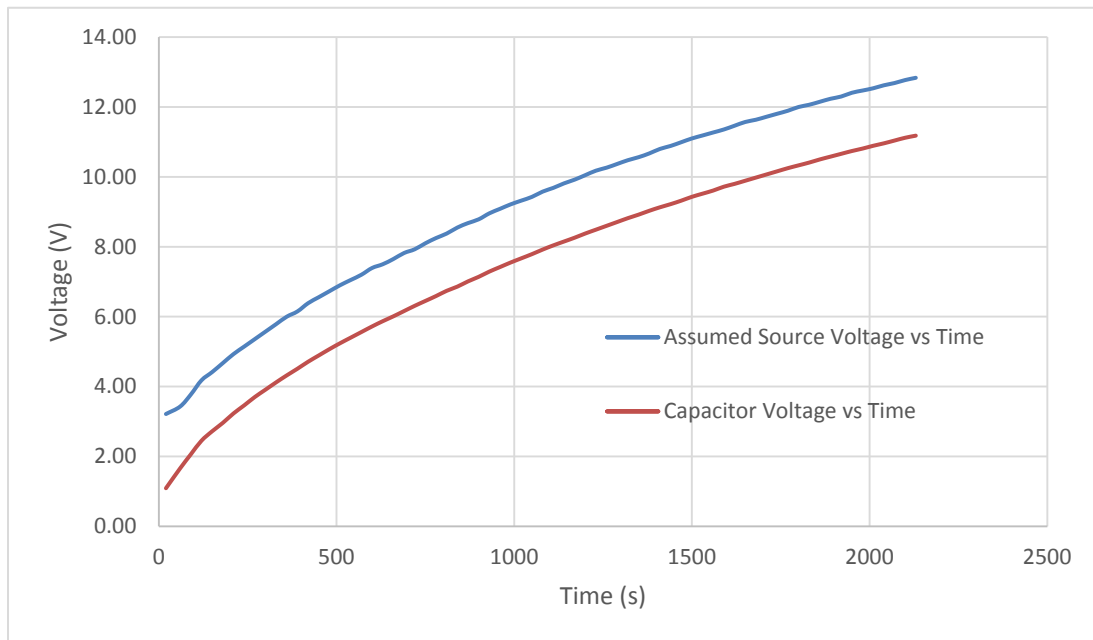
Figure 20.   Comparison of Assumed Source Voltage and Recorded DC Voltage
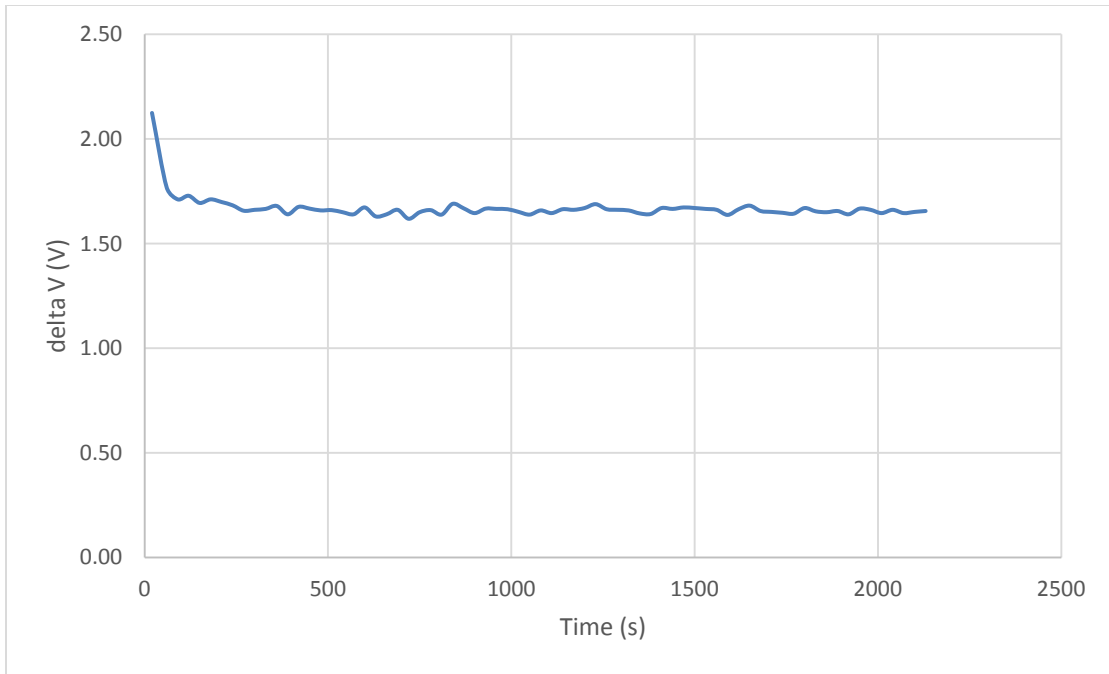
Figure 21. Difference between Assumed Voltage and Recorded Voltage

V. CONCLUSION

In conclusion, the goal of this thesis was to build a working demonstration of the concept of using compressed air as a working fluid to generate and store electrical energy. This goal was achieved by pairing two key enabling technologies to produce mechanical work which was then used to generate electricity. This project successfully demonstrated that small to medium scale energy storage can work by using compressed air. If the compressed air used in this project could be generated from renewable sources, a highly sustainable system could be implemented in a microgrid system which could improve the energy resiliency of naval installations.

THIS PAGE INTENTIONALLY LEFT BLANK

VI.   RECOMMENDATIONS

A.   REDESIGN THE TURBINE INLET

There is potential for improvement on the final design used for the compressed air interface with the turbine inlet. Utilizing the ejector concept to entrain air into the turbine inlet is a sure way to increase the shaft power output from the turbine. Additionally, a slightly larger turbocharger could also be used to increase the shaft power going to the motor, the wheel diameter of the turbine used was only 53 mm, and Garrett produces a turbocharger with a turbine wheel diameter of up to 111.5 mm [11].

B.   USE A SMALLER CAPACITOR

Although the current setup successfully charged the chosen supercapacitor to 15 volts, the time it took to get to that voltage was far too long to make it a feasible option for implementation. If a smaller capacitor were to be used it could still be able to store enough energy to be used to offset the initial power draws associated with the startup of heavy equipment.

C.   INCORPORATE A TRANSFORMER

Another way to achieve the desired voltage on the capacitor would be to incorporate a transformer to step up the voltage to the desired level. Doing this would most likely affect the charging rate as the initial current would be lower.

D.   USE A DIFFERENT MOTOR

As mentioned previously, one of the reasons the helicopter motor was used was that it was already on hand. Care should be taken in selecting a different motor. Some key parameters to keep in mind are the KV value, the rated power, and the maximum RPM. If the power of the motor is too high, it runs the risk of supplying too much opposing torque to the turbine, which could cause it to stop spinning. If the maximum RPM is too low, the motor could burn up and stop generating voltage.

E.   GRIND DOWN THE COMPRESSOR BLADES

Although the compressor housing was removed to expose the turbine shaft, the compressor was left on. There were two reasons for this. First, the compressor disk appeared to be threaded onto the shaft, which made it very difficult to remove without causing damage to the turbine. Second, the disk served to balance the shaft in the axial direction, which meant there was no variation in the tip gap between the turbine and the turbine housing. However, the compressor also used some of the shaft power coming from the turbine. If the blades could be ground down there would be more shaft work available to spin the motor.

F.   ENTRAIN WARMER AIR

The twofold effect of entraining air into the inlet produced an appreciable increase in shaft power. If low-grade or waste heat could be incorporated into the design to warm the air being entrained then the effectiveness of the turbine should increase.

G.   DESIGN A TURBINE SPECIFICALLY FOR THIS PURPOSE

Even though using an automobile turbocharger worked well for this project, more shaft power may be able to be produced from a turbine designed specifically for use with compressed air. This would of course include the design for a shaft and bearing system, as well as a housing for the turbine. This would bring this research closer to a final product.

APPENDIX A. ANSYS CFX MODELING OF TURBINE INLET

ANSYS Report

Date: 2016/12/07 12:32:20

_____
_____

Contents
1. Mesh Report
     Table 1 Mesh Information for CFX
2. Physics Report
     Table 2 Domain Physics for CFX
     Table 3 Boundary Physics for CFX

_____
_____

1. Mesh Report

Table 1. Mesh Information for CFX
Domain   Nodes Elements
Default Domain   292941   1661670

2. Physics Report

Table 2. Domain Physics for CFX
Domain - Default Domain
Type   Fluid
Location   B513
Materials
Air Ideal Gas
     Fluid Definition   Material Library
     Morphology   Continuous Fluid
Settings
Buoyancy Model   Non Buoyant
Domain Motion   Stationary
Reference Pressure 1.0000e+00 [atm]
Heat Transfer Model   Total Energy

Include Viscous Work Term   On
Turbulence Model   k epsilon
Turbulent Wall Functions   Scalable
    High Speed Model   Off

Table 3. Boundary Physics for CFX
Domain   Boundaries
Default Domain   Boundary - inlet front
        Type   INLET
        Location   inlet front
        Settings
        Flow Regime Mixed
            Blend Mach Number Type   Normal Speed
        Heat Transfer   Total Temperature
            Total Temperature   0.0000e+00 [C]
        Mass And Momentum   Normal Speed and Total Pressure
            Normal Speed   3.4600e+02 [m s^-1]
            Relative Total Pressure 1.0000e+02 [psi]
        Turbulence   Medium Intensity and Eddy Viscosity Ratio
        Boundary - inlet 1
        Type   OPENING
        Location   inlet 1
        Settings
        Flow Regime Subsonic
        Heat Transfer   Opening Temperature
            Opening Temperature   2.5000e+01 [C]
        Mass And Momentum   Entrainment
            Relative Pressure   0.0000e+00 [psi]
            Pressure Option Opening Pressure
        Turbulence   Zero Gradient
        Boundary - inlet 2
        Type   OPENING
        Location   inlet 2
        Settings
        Flow Regime Subsonic
        Heat Transfer   Opening Temperature
            Opening Temperature   2.5000e+01 [C]
        Mass And Momentum   Entrainment
            Relative Pressure   0.0000e+00 [psi]
            Pressure Option Opening Pressure
        Turbulence   Zero Gradient
        Boundary - inlet 3
        Type   OPENING
        Location   inlet 3

Settings
Flow Regime Subsonic
Heat Transfer   Opening Temperature
     Opening Temperature   2.5000e+01 [C]
Mass And Momentum   Entrainment
     Relative Pressure   0.0000e+00 [psi]
     Pressure Option Opening Pressure
Turbulence   Zero Gradient
Boundary - inlet 4
Type   OPENING
Location   inlet 4
Settings
Flow Regime Subsonic
Heat Transfer   Opening Temperature
     Opening Temperature   2.5000e+01 [C]
Mass And Momentum   Entrainment
     Relative Pressure   0.0000e+00 [psi]
     Pressure Option Opening Pressure
Turbulence   Zero Gradient
Boundary - outlet
Type   OPENING
Location   outlet
Settings
Flow Direction   Normal to Boundary Condition
Flow Regime Subsonic
Heat Transfer   Opening Temperature
     Opening Temperature   2.5000e+01 [C]
Mass And Momentum   Opening Pressure and Direction
     Relative Pressure   0.0000e+00 [psi]
Turbulence   Medium Intensity and Eddy Viscosity Ratio
Boundary - Default Domain Default
Type   WALL
Location   "F747.513,   F748.513,   F749.513,   F750.513,   F751.513,
F752.513, F753.513, F754.513, F755.513, F756.513, F757.513, F758.513,
F759.513, F760.513, F761.513, F762.513, F763.513, F764.513, F765.513,
F766.513, F767.513"
Settings
Heat Transfer   Adiabatic
Mass And Momentum   No Slip Wall
Wall Roughness   Smooth Wall

Figure 22.   Solidworks Model of the Turbine Housing Inlet
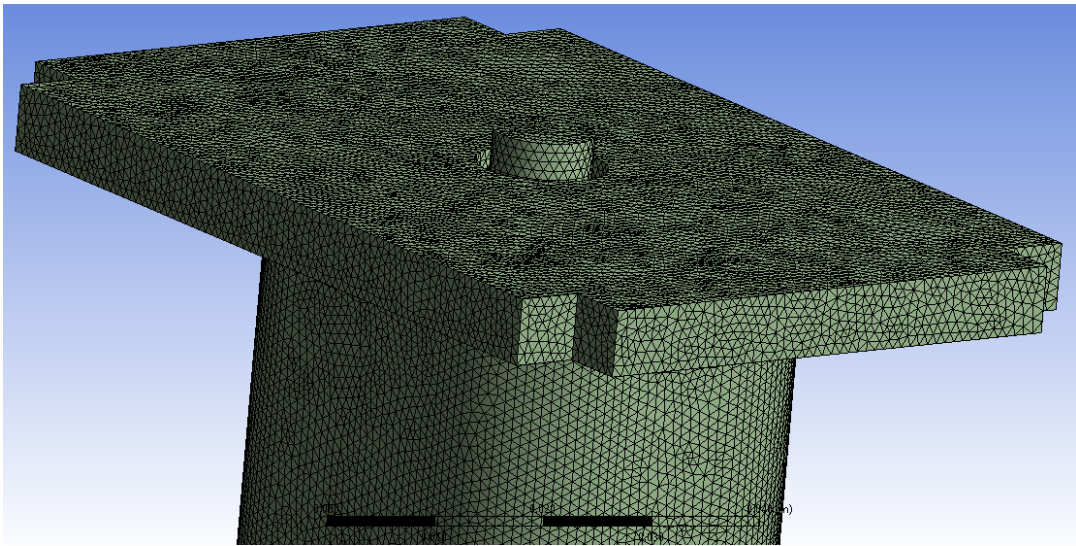
Figure 23.   Meshed Fluid Domain
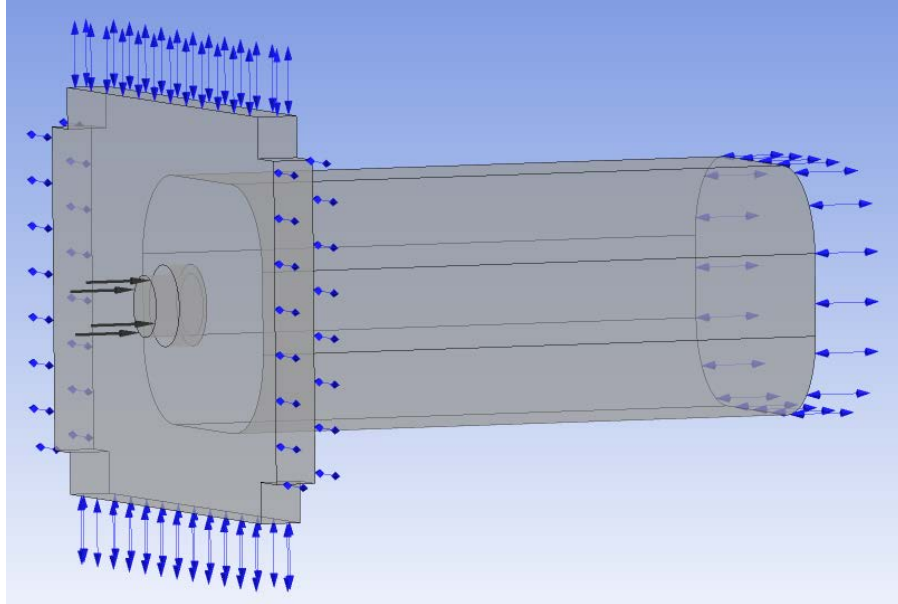
Figure 24.   Boundary Conditions
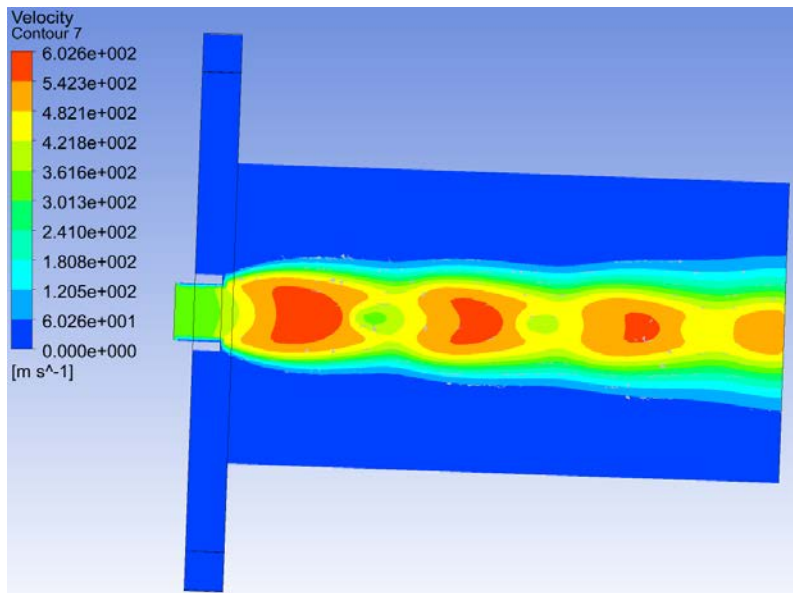
Figure 25.   Velocity Contours
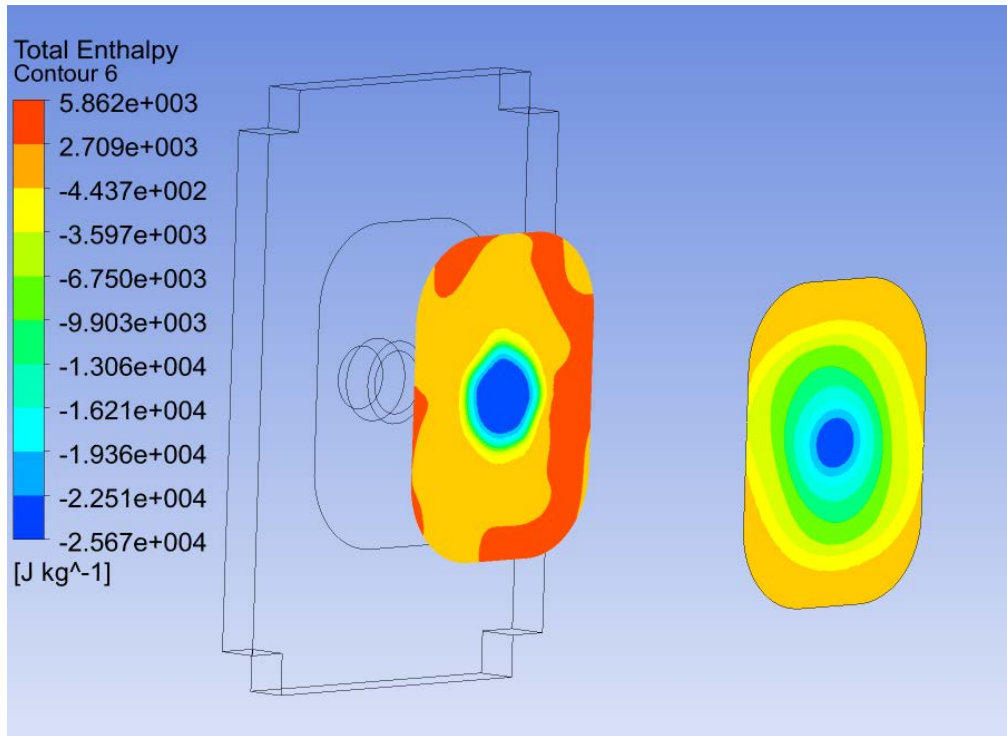
Figure 26.   Total Enthalpy Contours
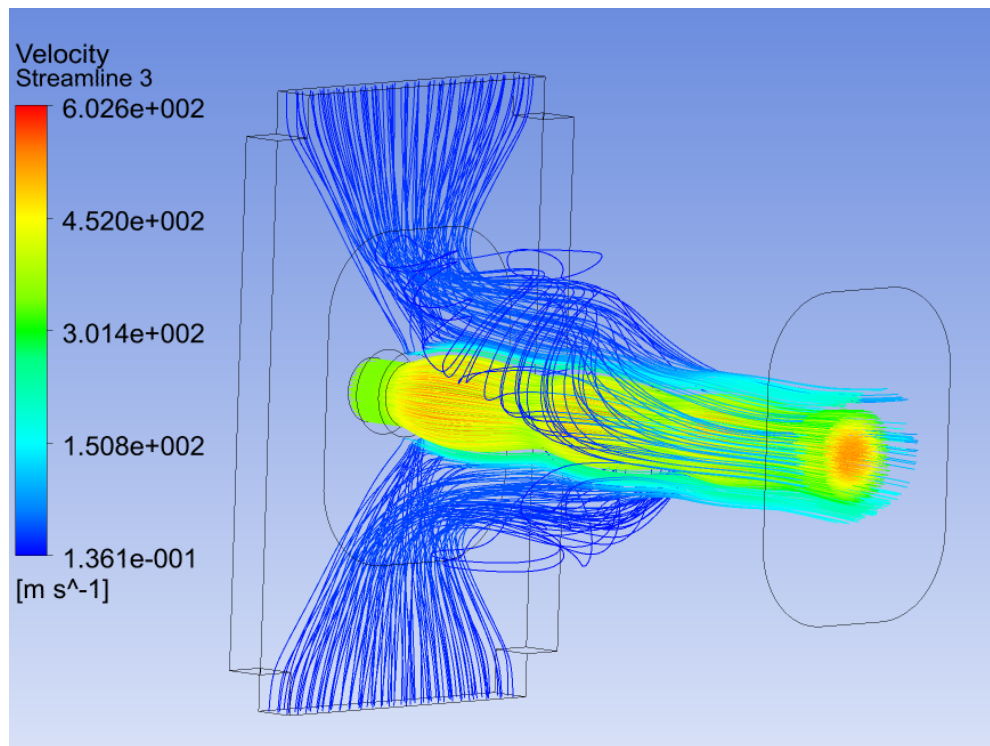
Figure 27.   Streamlines from Inlet and Two Openings
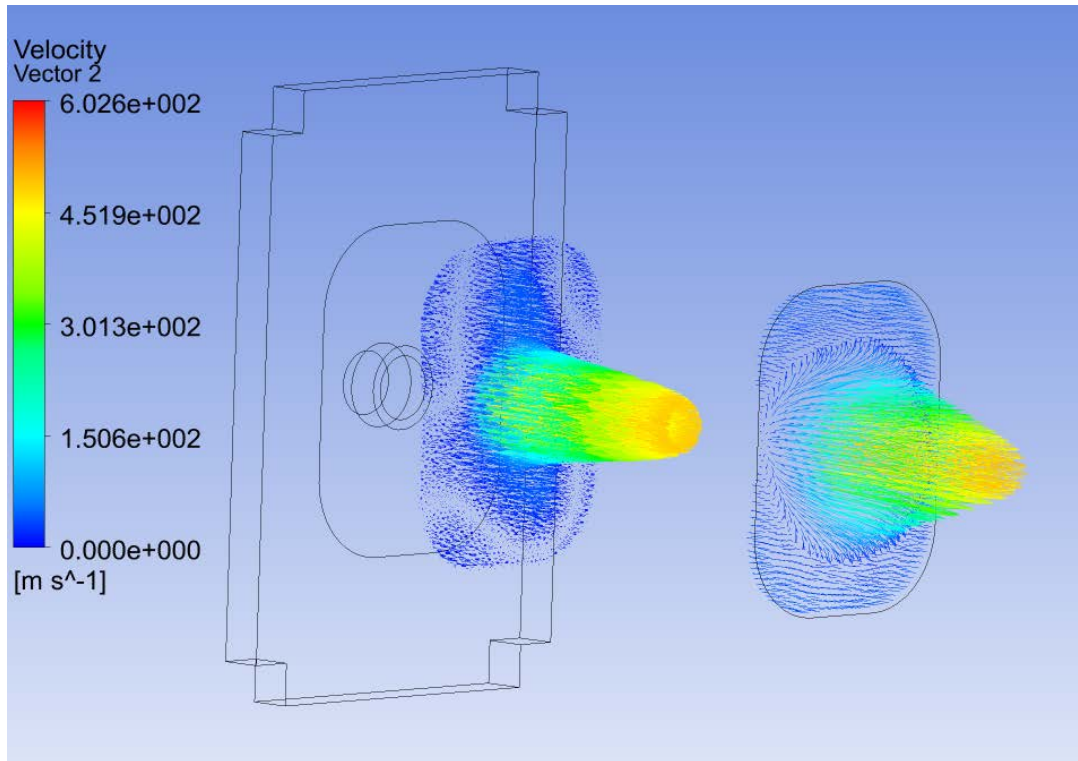
Figure 28.   Velocity Vectors

THIS PAGE INTENTIONALLY LEFT BLANK

APPENDIX B. TABULATED DATA FROM CHARGING CYCLE 1

Time (s)	Voltage (V)	Freq (Hz)	RPM	Possible Source Voltage	Voltage Difference	Energy Stored	Current
0	0	0					0
10	1					250	50.00
20	1.09	150	1800	3.21	2.12	297.025	4.50
60	1.66	160	1920	3.43	1.77	688.9	7.13
90	2.06	176	2112	3.77	1.71	1060.9	6.67
120	2.45	195	2340	4.18	1.73	1500.625	6.50
150	2.72	206	2472	4.41	1.69	1849.6	4.50
180	2.96	218	2616	4.67	1.71	2190.4	4.00
210	3.23	230	2760	4.93	1.70	2608.225	4.50
240	3.46	240	2880	5.14	1.68	2992.9	3.83
270	3.7	250	3000	5.36	1.66	3422.5	4.00
300	3.91	260	3120	5.57	1.66	3822.025	3.50
330	4.12	270	3240	5.79	1.67	4243.6	3.50
360	4.32	280	3360	6.00	1.68	4665.6	3.33
390	4.51	287	3444	6.15	1.64	5085.025	3.17
420	4.71	298	3576	6.39	1.68	5546.025	3.33
450	4.89	306	3672	6.56	1.67	5978.025	3.00
480	5.07	314	3768	6.73	1.66	6426.225	3.00
510	5.24	322	3864	6.90	1.66	6864.4	2.83
540	5.4	329	3948	7.05	1.65	7290	2.67
570	5.56	336	4032	7.20	1.64	7728.4	2.67
600	5.72	345	4140	7.39	1.67	8179.6	2.67
630	5.87	350	4200	7.50	1.63	8614.225	2.50
660	6.01	357	4284	7.65	1.64	9030.025	2.33
690	6.16	365	4380	7.82	1.66	9486.4	2.50
720	6.31	370	4440	7.93	1.62	9954.025	2.50
750	6.45	378	4536	8.10	1.65	10400.625	2.33
780	6.59	385	4620	8.25	1.66	10857.025	2.33
810	6.74	391	4692	8.38	1.64	11356.9	2.50
840	6.86	399	4788	8.55	1.69	11764.9	2.00
870	7.01	405	4860	8.68	1.67	12285.025	2.50
900	7.14	410	4920	8.79	1.65	12744.9	2.17
930	7.29	418	5016	8.96	1.67	13286.025	2.50
960	7.42	424	5088	9.09	1.67	13764.1	2.17
990	7.55	430	5160	9.21	1.66	14250.625	2.17
1020	7.67	435	5220	9.32	1.65	14707.225	2.00
1050	7.79	440	5280	9.43	1.64	15171.025	2.00
1080	7.92	447	5364	9.58	1.66	15681.6	2.17
1110	8.04	452	5424	9.69	1.65	16160.4	2.00
1140	8.15	458	5496	9.81	1.66	16605.625	1.83
1170	8.26	463	5556	9.92	1.66	17056.9	1.83
1200	8.38	469	5628	10.05	1.67	17556.1	2.00
1230	8.49	475	5700	10.18	1.69	18020.025	1.83
1260	8.6	479	5748	10.26	1.66	18490	1.83

Time (s)	Voltage (V)	Freq (Hz)	RPM	Possible Source Voltage	Voltage Difference	Energy Stored	Current
1290	8.71	484	5808	10.37	1.66	18966.025	1.83
1320	8.82	489	5868	10.48	1.66	19448.1	1.83
1350	8.92	493	5916	10.56	1.64	19891.6	1.67
1380	9.03	498	5976	10.67	1.64	20385.225	1.83
1410	9.13	504	6048	10.80	1.67	20839.225	1.67
1440	9.22	508	6096	10.89	1.67	21252.1	1.50
1470	9.32	513	6156	10.99	1.67	21715.6	1.67
1500	9.43	518	6216	11.10	1.67	22231.225	1.83
1530	9.52	522	6264	11.19	1.67	22657.6	1.50
1560	9.61	526	6312	11.27	1.66	23088.025	1.50
1590	9.72	530	6360	11.36	1.64	23619.6	1.83
1620	9.8	535	6420	11.46	1.66	24010	1.33
1650	9.89	540	6480	11.57	1.68	24453.025	1.50
1680	9.98	543	6516	11.64	1.66	24900.1	1.50
1710	10.07	547	6564	11.72	1.65	25351.225	1.50
1740	10.16	551	6612	11.81	1.65	25806.4	1.50
1770	10.25	555	6660	11.89	1.64	26265.625	1.50
1800	10.33	560	6720	12.00	1.67	26677.225	1.33
1830	10.41	563	6756	12.06	1.65	27092.025	1.33
1860	10.5	567	6804	12.15	1.65	27562.5	1.50
1890	10.58	571	6852	12.24	1.66	27984.1	1.33
1920	10.66	574	6888	12.30	1.64	28408.9	1.33
1950	10.74	579	6948	12.41	1.67	28836.9	1.33
1980	10.81	582	6984	12.47	1.66	29214.025	1.17
2010	10.89	585	7020	12.54	1.65	29648.025	1.33
2040	10.96	589	7068	12.62	1.66	30030.4	1.17
2070	11.04	592	7104	12.69	1.65	30470.4	1.33
2100	11.12	596	7152	12.77	1.65	30913.6	1.33
2130	11.18	599	7188	12.84	1.66	31248.1	1.00

APPENDIX C. TABULATED DATA FROM CHARGING CYCLE 2

Time (s)	VDC (V)	Frequency (Hz)	RPM	Energy Stored	Current
0	0	0	0	0	0.00
30	0.46	110.5	1326	52.9	7.67
60	0.72	123.1	1477	129.6	4.33
90	1.03	134.9	1619	265.225	5.17
120	1.34	147.1	1765	448.9	5.17
150	1.62	162.6	1951	656.1	4.67
180	1.9	173.96	2088	902.5	4.67
210	2.17	185.4	2225	1177.225	4.50
240	2.43	199.4	2393	1476.225	4.33
270	2.69	208.7	2504	1809.025	4.33
300	2.91	217.8	2614	2117.025	3.67
330	3.14	227.8	2734	2464.9	3.83
360	3.36	237.9	2855	2822.4	3.67
390	3.59	251.1	3013	3222.025	3.83
420	3.79	257.7	3092	3591.025	3.33
450	4.02	269.97	3240	4040.1	3.83
480	4.2	275.3	3304	4410	3.00
510	4.39	284.3	3412	4818.025	3.17
540	4.58	290.95	3491	5244.1	3.17
570	4.75	303.3	3640	5640.625	2.83
600	4.93	311.3	3736	6076.225	3.00
630	5.1	318.1	3817	6502.5	2.83
660	5.26	325.6	3907	6916.9	2.67
690	5.44	331.98	3984	7398.4	3.00
720	5.59	341.6	4099	7812.025	2.50
750	5.75	348.3	4180	8265.625	2.67
780	5.9	352.6	4231	8702.5	2.50
810	6.05	361.4	4337	9150.625	2.50
840	6.2	367.01	4404	9610	2.50
870	6.34	375.3	4504	10048.9	2.33
900	6.48	382.7	4592	10497.6	2.33
930	6.62	388.4	4661	10956.1	2.33
960	6.76	396.5	4758	11424.4	2.33
990	6.89	400.4	4805	11868.025	2.17
1020	7.02	407.9	4895	12320.1	2.17
1050	7.15	412.01	4944	12780.625	2.17
1080	7.26	418.7	5024	13176.9	1.83
1110	7.39	425.7	5108	13653.025	2.17
1140	7.51	428.4	5141	14100.025	2.00
1170	7.64	435.1	5221	14592.4	2.17
1200	7.75	441.95	5303	15015.625	1.83
1230	7.87	448.6	5383	15484.225	2.00
1260	7.98	452.9	5435	15920.1	1.83
1290	8.09	456.3	5476	16362.025	1.83
1320	8.2	463.1	5557	16810	1.83
1350	8.31	467.7	5612	17264.025	1.83

Time (s)	VDC (V)	Frequency (Hz)	RPM	Energy Stored	Current
1380	8.41	472.04	5664	17682.025	1.67
1410	8.52	477.8	5734	18147.6	1.83
1440	8.62	482.1	5785	18576.1	1.67
1470	8.75	488.5	5862	19140.625	2.17
1500	8.82	489.5	5874	19448.1	1.17
1530	8.92	496.01	5952	19891.6	1.67
1560	9.03	500.06	6001	20385.225	1.83
1590	9.12	504.6	6055	20793.6	1.50
1620	9.21	509.7	6116	21206.025	1.50
1650	9.3	513.6	6163	21622.5	1.50
1680	9.4	516.7	6200	22090	1.67
1710	9.49	523.3	6280	22515.025	1.50
1740	9.58	522.5	6270	22944.1	1.50
1770	9.66	530.3	6364	23328.9	1.33
1800	9.75	535.9	6431	23765.625	1.50
1830	9.83	534.9	6419	24157.225	1.33
1860	9.91	540.98	6492	24552.025	1.33
1890	10.02	546.05	6553	25100.1	1.83
1920	10.07	549.4	6593	25351.225	0.83
1950	10.15	550.6	6607	25755.625	1.33
1980	10.23	554.3	6652	26163.225	1.33
2010	10.3	559.2	6710	26522.5	1.17
2040	10.38	565.4	6785	26936.1	1.33
2070	10.45	563.2	6758	27300.625	1.17
2100	10.52	570.01	6840	27667.6	1.17
2130	10.59	571.7	6860	28037.025	1.17
2160	10.66	574.4	6893	28408.9	1.17
2190	10.73	580.2	6962	28783.225	1.17
2220	10.79	582.1	6985	29106.025	1.00
2250	10.86	582.3	6988	29484.9	1.17
2280	10.91	586.8	7042	29757.025	0.83
2310	10.99	591.2	7094	30195.025	1.33
2340	11.05	592.7	7112	30525.625	1.00
2370	11.11	598.3	7180	30858.025	1.00
2400	11.18	599.5	7194	31248.1	1.17
2430	11.24	602.8	7234	31584.4	1.00
2460	11.3	606.8	7282	31922.5	1.00
2490	11.36	607.4	7289	32262.4	1.00
2520	11.42	611.97	7344	32604.1	1.00
2550	11.48	614.5	7374	32947.6	1.00
2580	11.53	616.2	7394	33235.225	0.83
2610	11.58	617.6	7411	33524.1	0.83
2640	11.64	619.5	7434	33872.4	1.00
2670	11.69	621.5	7458	34164.025	0.83
2700	11.73	625.5	7506	34398.225	0.67

LIST OF REFERENCES

[1]   Darwish, A., and Boehm, R.F., 2011, "Compressed Air Energy Storage Flow And Power Analysis," *Proc. ASME 5th International Conference on Energy Sustainability*, Washington, DC, p. 2.

[2]   Deputy Assistant Secretary of the Navy Energy Office, 2012, "Department of the Navy Strategy for Renewable Energy," Department of the Navy, Washington, DC.

[3]   Barnhart, C.J., and Benson, S.M., 2013, "On the Importance of Reducing the Energetic and Material Demands of Electrical Energy Storage," *Energy and Environmental Science*, **6**, p.1086.

[4]   Pollman, A.G., and Gannon, A.J., 2015, "Multi-Physics Approach & Demonstration Facility," ES2015-49084, *Proc. ASME 9th International Conference on Energy Sustainability*, San Diego, CA, p. 3.

[5]   Energy Storage Association, n.d., "Compressed Air Energy Storage," from http://energystorage.org/compressed-air-energy-storage-caes

[6]   Petrov, M.P., Arghandeh, R., Broadwater, R., 2013, "Concept And Application Of Distributed Compressed Air Energy Storage Systems Integrated In Utility Networks," *Proceedings of the ASME 2013 Power Conference*, 2013, Boston, MA, p. 2.

[7]   Magneti Marelli, n.d., "KERS (Kinetic Energy Recovery System," http://www.magnetimarelli.com/excellence/technological-excellences/kers

[8]   White, F.M., 2011, *Fluid Mechanics*, McGraw Hill, New York, NY, Chaps. 9, 11.

[9]   Presz, W., and Blinn, R.F., 1987, "Short Efficient Ejector Systems," *AIAA/SAE/ASME/ASEE 23rd Joint Propulsion Conference*, San Diego, CA, pp. 1–3.

[10]   Kuphaldt, T.R., 2007, *Lessons in Electric Circuits, Volume II-AC*, All About Circuits, Boise, ID, Chaps. 1, 9, 13.

[11]   Garrett by Honeywell, 2016, "Turbocharger Guide," 5, Honeywell Turbo Technologies, Torrance, CA.

[12]   Scorpion Power System Ltd., n.d., "Scorpion HKIII-4035-560KV," http://www.scorpionsystem.com/catalog/helicopter/motors_4/hkiii-40_1/hkiii-4035/HKIII_4035_560/

[13]   Kuphaldt, T.R., 2009, *Lessons in Electric Circuits, Volume III-Semiconductors*, All About Circuits, Boise, ID, Chap. 3.

[14]   Mouser Electronics, n.d., "IXYS VUO86-16NO7," http://www.mouser.com/ProductDetail/IXYS/VUO86-16NO7/?qs=sGAEpiMZZMtQ8nqTKtFS%2fKGlmTW84eZIUC9Sdod6eh8%3d

[15]   IXYS, 2013, "VUO86-16NO7 Product Information," IXYS, Milpitas, CA.

[16]   Maxwell Technologies, 2016, "16 Volt Large Module," http://www.maxwell.com/products/ultracapacitors/16v-large-modules

[17]   Kuphaldt, T.R., 2009, *Lessons in Electric Circuits, Volume I-DC*, All About Circuits, Boise, ID, Chap. 13.

[18]   Plonus, M.A., 1978, *Applied Electromagnetics*, McGraw Hill, Singapore, Chap. 5.

INITIAL DISTRIBUTION LIST

1.   Defense Technical Information Center
        Ft. Belvoir, Virginia

2.   Dudley Knox Library
        Naval Postgraduate School
        Monterey, California